Modeling molecular effects on plasmon transport: Silver nanoparticles with tartrazine

Christopher Arntsen, Kenneth Lopata, Michael R. Wall, Lizette Bartell, and Daniel Neuhauser[a)]
Department of Chemistry and Biochemistry, University of California, Los Angeles, California 90095-1569, USA

(Received 22 July 2010; accepted 23 December 2010; published online 23 February 2011)

Modulation of plasmon transport between silver nanoparticles by a yellow fluorophore, tartrazine, is studied theoretically. The system is studied by combining a finite-difference time-domain Maxwell treatment of the electric field and the plasmons with a time-dependent parameterized method number 3 simulation of the tartrazine, resulting in an effective Maxwell/Schrödinger (i.e., classical/quantum) method. The modeled system has three linearly arranged small silver nanoparticles with a radius of 2 nm and a center-to-center separation of 4 nm; the molecule is centered between the second and third nanoparticles. We initiate an *x*-polarized current on the first nanoparticle and monitor the transmission through the system. The molecule rotates much of the *x*-polarized current into the *y*-direction and greatly reduces the overall transmission of *x*-polarized current. © *2011 American Institute of Physics*. [doi:10.1063/1.3541820]

I. INTRODUCTION

Plasmonic materials,[1,2] where electrons oscillate collectively, are interesting to study due to a wide range of properties. Plasmon frequencies are tunable by modifying size,[3] shape,[4] and geometry.[5] The propagation and transmission of surface plasmons through plasmonic materials can be specifically modulated,[6] including subwavelength focusing of electromagnetic energy.[7] Plasmonic materials also generate highly intense fields at their surfaces when excited,[1] resulting in a strong interaction with neighboring molecules.[8] The most common example is surface enhanced Raman spectroscopy, where intense fields lead to very sensitive measurements (up to 15 orders of magnitude more sensitive than that of the traditional Raman spectroscopy).[9] Recently, chlorophyll has been shown to have an 18-fold increase in fluorescence as a result of plasmon interactions when placed near a silver surface.[10]

Given the intensity of the fields surrounding excited plasmonic materials, it is not surprising that these materials have a strong effect on neighboring molecules. It is remarkable that a few[11] or even individual molecules can also greatly affect a plasmonic material. We have recently shown that two-level molecules can rotate plasmon polarization transmitted between nearby nanoparticles as well as greatly affect the energy transmission.[12] To expand this work, we investigate the effect of a large fluorophore having a strong transition dipole moment on the polarization and transmission of current through similar arrays of metal nanoparticles.

In previous papers[12,13] on a two-level molecule, we showed that for a pronounced effect on the polarization and transmission of current through metal nanoparticles to occur, the molecule must have an excitation energy similar to the plasmon resonance frequency of the metal. Here, we investigate the effects on silver nanoparticles, and therefore chose a yellow fluorophore, tartrazine (Fig. 1), as its excitation energy is similar to the plasmon resonance frequency of silver. While Ref. 12 studies a similar system with a two-level model for the molecule, a more thorough study is warranted. Two-level systems could have vastly different properties in principle; primarily, this is because each time the molecule is excited it relaxes to the same ground level. A realistic description of a molecule, with its variety of excited states and a wide absorption profile could yield very different results, which, *a priori*, could have masked the effect. Fortunately, as we show below, this is not the case, and a strong molecular effect remains.

On the length scales relevant to metal nanoparticles, metal electrons can be well treated classically.[14] We thus employ the finite-difference time-domain (FDTD) method, which has been shown to accurately model metal nanoparticles.[15] The molecule was subsequently modeled using time-dependent parameterized method number 3 (TDPM3), a time-dependent version of a semiempirical quantum mechanical routine.[16] TDPM3 was chosen over more common methods such as time-dependent density functional theory (TDDFT) as it is significantly faster.

TDPM3 has recently been shown to fairly accurately model large organic molecules, yielding excitation energies within 15% of experiment and TDDFT.[17] The method is very efficient because of the ease of applying the Fock operator and the small (minimal) basis set. Thus, TDPM3 allows the simulation of large fluorophores, which have a strong transition dipole moment.

The resulting simulations, discussed below, show that a single molecule can sufficiently modify the transmitted current and rotate its direction to potentially conceive devices that could measure such a change in the *y*-polarized current and give single molecule detection. Further, future

a)Author to whom correspondence should be addressed. Electronic mail: dxn@chem.ucla.edu.

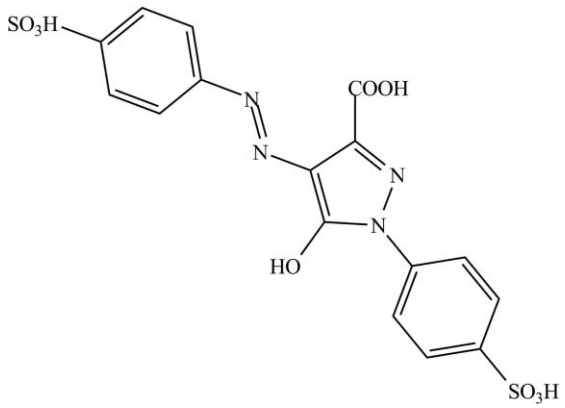

FIG. 1. The yellow fluorophore tartrazine as oriented in this work.

simulations will investigate how plasmon propagation can be modified by a larger set of molecules.

Section II A describes the FDTD method used to model the silver nanoparticles, Sec. II B the TDPM3 method used for the molecule, and Sec. II C the interaction between the two. Section III describes the investigated system and discusses the results. Conclusions follow in Sec. IV.

II. THEORY

A. Classical treatment

To treat the metal and vacuum background classically, we set interlocking Yee grids to describe the electric field, magnetic field, and plasmon generated current.[14] To avoid double counting of the self-interaction of the molecule (beyond the inherent Coulomb integrals in the time-dependent TDPM3 Hamiltonian), we also establish such grids for a separate molecule-induced field, so that the molecule is only influenced by the external field and by the TDPM3 Hamiltonian, and not by its induced electric field.

We label the fields generated by the molecule with subscript m and the fields generated by the plasmons with subscript p. Thus, the total fields are (see Ref. 12)

$$\boldsymbol{E}_{\text{tot}}(\boldsymbol{r},t) = \boldsymbol{E}_p(\boldsymbol{r},t) + \boldsymbol{E}_m(\boldsymbol{r},t), \tag{1}$$

$$\boldsymbol{H}_{\text{tot}}(\boldsymbol{r},t) = \boldsymbol{H}_p(\boldsymbol{r},t) + \boldsymbol{H}_m(\boldsymbol{r},t), \tag{2}$$

$$\boldsymbol{J}_{\text{tot}}(\boldsymbol{r},t) = \boldsymbol{J}_p(\boldsymbol{r},t) + \boldsymbol{J}_m(\boldsymbol{r},t). \tag{3}$$

The total fields are defined and evolved in time in terms of the Maxwell equations:

$$\frac{\partial \boldsymbol{E}_{\text{tot}}(\boldsymbol{r},t)}{\partial t} = \frac{1}{\varepsilon_{\text{eff}}(\boldsymbol{r})}\left[\nabla \times \boldsymbol{H}_{\text{tot}}(\boldsymbol{r},t) - \boldsymbol{J}_{\text{tot}}(\boldsymbol{r},t)\right], \tag{4}$$

$$\frac{\partial \boldsymbol{H}_{\text{tot}}(\boldsymbol{r},t)}{\partial t} = -\frac{1}{\mu_0}\nabla \times \boldsymbol{E}_{\text{tot}}(\boldsymbol{r},t). \tag{5}$$

The plasmonic current is calculated as (Ref. 14)

$$\frac{\partial \boldsymbol{J}_p(\boldsymbol{r},t)}{\partial t} = \alpha(\boldsymbol{r})\,\boldsymbol{J}_p(\boldsymbol{r},t) + \beta(\boldsymbol{r})\,\boldsymbol{E}_{\text{tot}}(\boldsymbol{r},t), \tag{6}$$

where, as usual, the metal susceptibility functions, ε_{eff}, α, and β are defined according to

$$\varepsilon_{\text{eff}}(\boldsymbol{r}) = \varepsilon_0 \varepsilon_{r,\infty}(\boldsymbol{r}), \tag{7}$$

$$\alpha(\boldsymbol{r}) = -\gamma_D(\boldsymbol{r}), \tag{8}$$

$$\beta(\boldsymbol{r}) = \varepsilon_0[\omega_D(\boldsymbol{r})]^2. \tag{9}$$

$\varepsilon_{r,\infty}(\boldsymbol{r})$, $\gamma_D(\boldsymbol{r})$, and ω_D are the Drude asymptotic relative permittivity, damping constant, and plasma frequency, respectively. The parameters are material dependent, and fitted to experimental values[14,15,18] (parameters used in the simulations were taken from Ref. 18).

The plasmonic fields are evolved in time by the Maxwell equations:

$$\frac{\partial \boldsymbol{E}_p}{\partial t} = \frac{1}{\varepsilon_{\text{eff}}}\nabla \times \boldsymbol{H}_p + \left(\frac{1}{\varepsilon_{\text{eff}}} - \frac{1}{\varepsilon_0}\right)\nabla \times \boldsymbol{H}_m - \frac{1}{\varepsilon_{\text{eff}}}\boldsymbol{J}_p, \tag{10}$$

$$\frac{\partial \boldsymbol{H}_p}{\partial t} = -\frac{1}{\mu_0}\nabla \times \boldsymbol{E}_p. \tag{11}$$

Note that Eq. (10) has a contribution from the molecular magnetic field, unlike Eq. (11). This is because the plasmon's electric field is the difference of the total and molecular components, and each of these is affected by a different susceptibility, leading to the term from the molecular magnetic field. As the magnetic susceptibility is assumed constant between the plasmons and the surrounding air, no such term exists for Eq. (11), which is therefore much simpler. The full derivation can be found in Ref. 12. The last ingredient is the molecular current, which is derived below from the quantum mechanical density matrix.

B. Quantum mechanical treatment

To model the contribution of the molecule, we employ the TDPM3 method.[17] TDPM3 is a semiempirical time-dependent method which greatly reduces the computational cost of modeling the molecule. TDPM3 gains efficiency in several ways. First, it treats the inner shell electrons of an atom and the nucleus as a fixed core, and thus only explicitly treats the valence electrons. Second, the PM3 Hamiltonian is defined in terms of parameterized variables, optimized to fit experimental data:

$$H_{\mu\mu} = U_{\mu\mu} + \sum_B V_{\mu\mu,B} \tag{12}$$

$$H_{\mu\nu} = \sum_B V_{\mu\nu,B} \tag{13}$$

$$H_{\mu\lambda} = \frac{1}{2}\left(\beta_\mu^A + \beta_\lambda^B\right) S_{\mu\lambda}. \tag{14}$$

Here, $U_{\mu\mu}$ corresponds to the sum of the kinetic energy of the electron in orbital μ and the potential energy resulting from the attraction of the electron in orbital μ and the core of the atom on which that orbital is located. $V_{\mu\nu,B}$ corresponds to the attraction of an electron in atom A to the core of atom B. The β values are parameters specific to the orbital type and atom. These parameters are typically fitted to spectroscopic

data. Finally, $S_{\mu\lambda}$ is an element of the overlap matrix. The β terms are used to describe the group state of a molecule.

Note that no image potential is used on the metal; formally, it will be required in a static or near static treatment, where the metal's reflectivity effect manifests itself as an image charge. However, we are interested at higher frequencies, where the metal is no longer a purely reflecting substance and instead its properties are explicitly accounted for by the Maxwell equation and the frequency dependent susceptibility.

The electric field is included by a usual dipole moment, as we ignore the effect of the magnetic field on the molecule:

$$H_{ij} = H_{0,ij} + \boldsymbol{E}_p \cdot \boldsymbol{d}_{ij}. \tag{15}$$

H_{ij} is a matrix element of the corrected, excited state Hamiltonian, $H_{0,ij}$ is the corresponding matrix element of the ground state Hamiltonian described above in Eqs. (12)–(14), $\boldsymbol{E}_p$ is the plasmon-induced electric field at the molecule's location, and $\boldsymbol{d}_{ij}$ is the dipole matrix of the molecule. The calculations are concerned with qualitative effects so that the inherent accuracy of TDPM3, about 15%–20% for excited states of organic molecule, is quite acceptable.

The Fock matrix in PM3 calculations is composed of the Hamiltonian and 2-electron terms only, and since 3- and 4-center contributions are neglected, the method is very efficient. The 1-center α (spin-up) Fock matrix is defined as

$$\begin{aligned} F^{\alpha}_{\mu\nu} = {} & H_{\mu\nu} + 2P^{\alpha+\beta}_{\mu\nu}\left(\phi^A_\mu\phi^A_\nu, \phi^A_\mu\phi^A_\nu\right) \\ & - P^{\alpha}_{\mu\nu}\left[\left(\phi^A_\mu\phi^A_\nu, \phi^A_\mu\phi^A_\nu\right) + \left(\phi^A_\mu\phi^A_\mu, \phi^A_\nu\phi^A_\nu\right)\right] \\ & + \sum_B \sum_{\lambda,\sigma} P^{\alpha+\beta}_{\lambda\sigma}(\phi^A_\mu\phi^A_\nu, \phi^B_\lambda\phi^B_\sigma), \end{aligned} \tag{16}$$

while the 2-center matrix elements are written as

$$F^{\alpha}_{\mu\lambda} = H_{\mu\lambda} - \sum_{\nu} \sum_{\sigma} P^{\alpha}_{\nu\sigma}\left(\phi^A_\mu\phi^A_\nu, \phi^B_\lambda\phi^B_\sigma\right). \tag{17}$$

Here, P is the density matrix, and we introduced the repulsion integrals of atomic orbitals ϕ of the specified atom. These repulsion integrals are semiempirically fitted to atomic properties (see Ref. 16). Note the inclusion of only 1- and 2-center integrals.

C. Interaction between molecule and FDTD grid

The interaction between the quantum-mechanically treated molecule and the classically treated metal nanoparticles is through the molecular current term, which is obtained

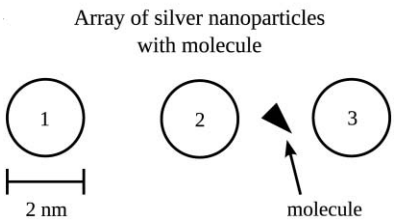

FIG. 2. The system studied consists of three silver nanoparticles, each with a 2 nm diameter and a center-to-center distance of 4 nm. The molecule is located halfway between the second and third nanoparticles.

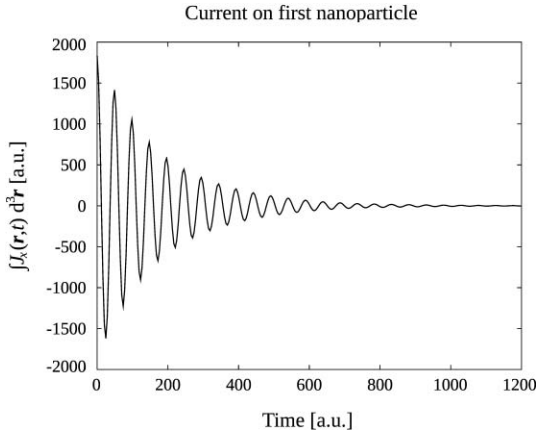

FIG. 3. The time-resolved x-polarized current on the first nanoparticle. The current is induced on the first nanoparticle with a pulse as from a tip, and transfers to the other nanoparticles via plasmon propagation.

from the von Neumann equation for the evolution of the density matrix:

$$\frac{dP}{dt} = -i\,[F(P),\, P] - \frac{P - P_0}{\tau}, \tag{18}$$

where F is the Fock matrix and $-(P - P_0)/\tau$ represents a phenomenological damping of the density matrix. Without this latter term, an excited molecule would only dissipate energy radiatively and would remain excited much longer than is physically reasonable.

We found that the transmitted current in Fourier space is insensitive to the value of the damping constant unless it is realistically too short (30 a.u., i.e., less than 1 fs, or lower). The reason is that almost all the transport happens on a very short time scale (the scale of transport from field to molecule and vice versa), so that the damping of the residual values of the current does not change its Fourier transform. Note that the overall dynamics takes reasonably long times (hundreds of atomic units, more than 10 fs, as presented later), but since

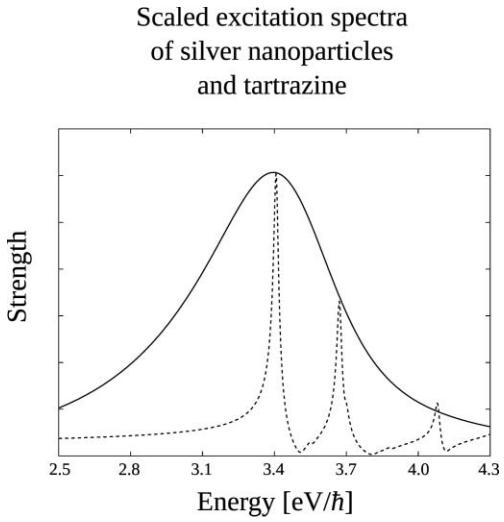

FIG. 4. Overlay of the silver plasmon resonance (solid line) and the absorption spectrum of tartrazine (dashed line). The silver plasmon resonance curve was generated using FDTD, and the absorption spectrum of tartrazine was generated using TDPM3.

TABLE I. The physical parameters of silver and the molecule used in the simulations. All values are in a.u.

Silver	Molecule
$\varepsilon_{r,\infty} = 5.976$	
$\gamma_D = 9.582 \times 10^{-3}$	$\tau = 30$
$\omega_D = 0.3630$	

the molecule mainly acts as a scatterer, only its short time dynamics is relevant; so there is no dependence on the damping constant.

Note that from Eq. (15) the Fock matrix includes the electric field. It should also be noted that the molecule and the grid act entirely through this current term, and that electrons are not actually shared between the two regimes.

The dipole moment $\boldsymbol{\mu}$ of the molecule is

$$\boldsymbol{\mu} = \sum_{ij} \boldsymbol{d}_{ij} \cdot P_{ij}, \tag{19}$$

and the current is calculated as

$$\boldsymbol{J}_m = \frac{\partial \boldsymbol{\mu}}{\partial t}. \tag{20}$$

The FDTD equations [Eqs. (4)–(6)] are solved simultaneously with the TDPM3 equations for the density matrix and the current [Eqs. (18) and (20)]. In practice, the evolution is done by alternating between an FDTD evolution of the electromagnetic fields and plasmonic current, and a TDPM3 evolution of the density matrix.

III. RESULTS

Figure 2 shows the basic setup. Plasmons are induced in the first nanoparticle (labeled 1) through adding a pulse of current (i.e., a delta function in time) as from a tip. The current is then propagated through the array via plasmon transfer as defined by the Maxwell equations, listed above in Sec. II A. Figure 3 shows the induced current on the first nanoparticle. While a 2 nm diameter metal sphere is very small, experimentally, we chose to use such a size in our investigation, as it is sufficiently small for a single molecule that has a strong effect. We investigated systems with a more experimentally common size of 5 nm, but the effect is diminished. Future work will examine the effect of using a set of molecules rather than a single one, on larger spheres.

The molecule used is tartrazine, shown in Fig. 1. We chose this molecule due to its strong transition dipole moment at 3.406 eV/$\hbar$, which is very close to the plasmon frequency of silver nanoparticles, 3.397 eV/$\hbar$ (Fig. 4). The molecule is oriented along the negative xy-axis as indicated in Fig. 1.

TABLE II. Time parameters used in simulations. All values are in a.u.

Grid	Time
$N_x = 150$	
$N_y = 50$	$dt = 0.006$
$N_z = 50$	$t_{\max} = 2024$
$dx = dy = dz = 2$	

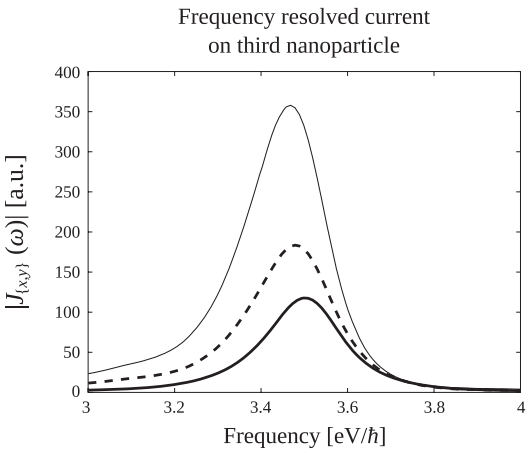

FIG. 5. Frequency resolved current on the third nanoparticle in the x-direction (solid lines) with (bold) and without (narrow) the molecule and in the y-direction with the molecule (dashed line). The presence of the molecule rotates the x-polarized current into the y-direction, resulting in a y-polarized current on the third nanoparticle.

The simulations used are given in Eqs. (1)–(6) and (10)–(20). The physical parameters can be found in Table I and the simulation parameters are in Table II. The time-step used was 0.006 a.u., and the total grid had 150 × 50 × 50 points, with a 2 a.u. grid spacing. Convergence with respect to the time-step, number of grid points, and grid spacing were confirmed.

Figure 5 shows the frequency resolved current on the third nanoparticle with and without the molecule. The molecule significantly reduces the current in the x-direction and increases the current in the y-direction.

The induced current on the molecule, shown in Fig. 6, effectively rotates the transferred current between the second nanoparticle and the third nanoparticle from the x-direction to the y-direction. This effect is a result of the strong transition dipole moment in tartrazine near the plasmonic frequency of silver. The molecule absorbs much of the current in the x-direction from the second nanoparticle and re-emits nearly all of the current in the y-direction.

We also investigated the effect of the molecular orientation of the molecule. Figure 7 shows the frequency resolved x- and y-currents on the molecule and on the third

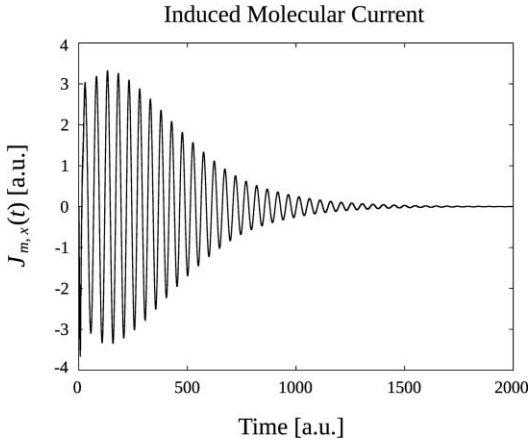

FIG. 6. The x-polarized current on the molecule as a function of time. The y-polarized current (not shown) is slightly larger than the x-polarized current.

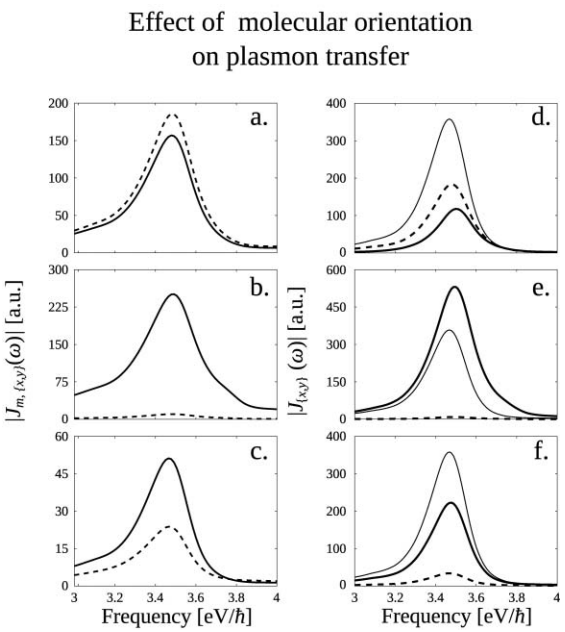

FIG. 7. (a)–(c) The x-polarized (solid line) and y-polarized (dashed line) currents of the molecule oriented along the xy-axis, x-axis, and y-axis, respectively. (d)–(f) The frequency resolved current on the third nanoparticle for each of these orientations. The x-polarized currents are represented with a solid line, and the y-polarized currents with a dashed line. The bold lines are for simulations with a molecule, and narrow lines are for simulations without a molecule. Note the different scales on the y-axes.

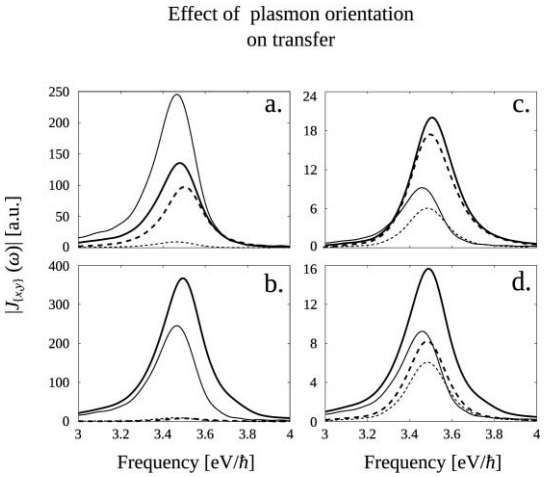

FIG. 8. (a) and (b) The frequency resolved current on the third nanoparticle for systems in which the initial current is oriented along the xy-axis for systems without the molecule (narrow lines) and with the molecule (bold line) oriented along the xy-axis (a) and x-axis (b). The x-polarized current is shown with a solid line, and the y-current with a dashed line. (c) and (d) Systems with an initial current in the y-direction, and a molecule oriented along the xy-axis and the x-axis. Note the different scale on the y-axes.

nanoparticle for systems with the molecule oriented along the xy-axis, the x-axis, and the y-axis. For a molecule oriented along the x-axis, the current on the molecule is entirely in the x-direction, and subsequently no y-oriented current is observed on the third nanoparticle. The x-polarized current in this orientation is very high, and actually results in an enhanced transfer from the second nanoparticle to the third, as shown in Fig. 7(e). For a y-oriented molecule, the current on the molecule is very small. The majority of the current is in the x-direction, but this current is negligible compared with the case that the molecule is oriented differently. The most interesting part is when the molecule is in the xy-direction. Then, one can either view the process as a molecule absorbing x-polarized radiation and then emitting xy-polarized current, or simply view it as a scattering process, as the molecule can only absorb and emit radiation in the xy-direction, so that the initial polarization of the light is projected to the molecular xy-direction.

Note the current on the third nanoparticle and on the molecule for the different orientations mentioned above. Specifically, when a molecule is oriented along the y-axis, very little energy is absorbed. The rotation of current in the nanoparticles is not just a function of the molecule's presence, but also the orientation, as it scatters the radiation.

We also investigated the effects of rotating the initial current on the first nanoparticle. In Figs. 8(a) and 8(b), we investigate systems with an initial current in the xy-direction and molecules in the xy- and x-directions, respectively. Notice that for systems without a molecule, almost no y-current is transmitted to the third nanoparticle; this is due to the fact that there is no mechanism to transmit y-current between the first and second nanoparticles. Thus, for systems with the molecule in the xy-direction, the molecule again rotates x-current into the y-direction. Likewise, the x-oriented molecule enhances the transmission of x-current, but has no effect on the y-current. For systems where the current is introduced in the y-direction, very little current reaches the third nanoparticle. In these cases, we observe similar behavior as before: the xy-oriented molecule rotates some current into the x-direction, and the x-oriented molecule enhances the transfer in the x-direction.

The molecule also has a strong effect on the energy transfer between the second and third nanoparticles. The transfer of the x-polarized current is defined as

$$T(\omega) = \left| \frac{J_{x,3}(\omega)}{J_{x,2}(\omega)} \right|. \tag{21}$$

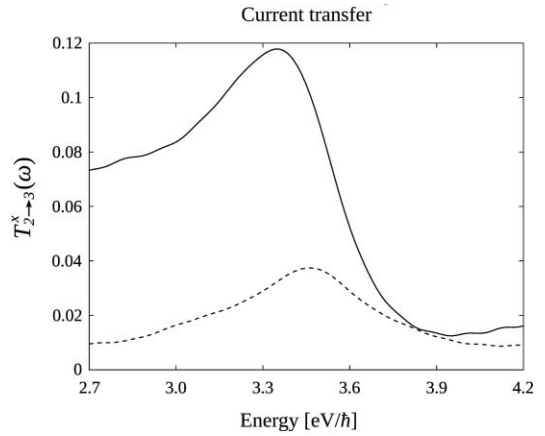

FIG. 9. The percentage of x-polarized current transfer from the second to the third nanoparticle without (solid line) and with (dashed line) a molecule. The presence of a molecule significantly reduced the x transfer.

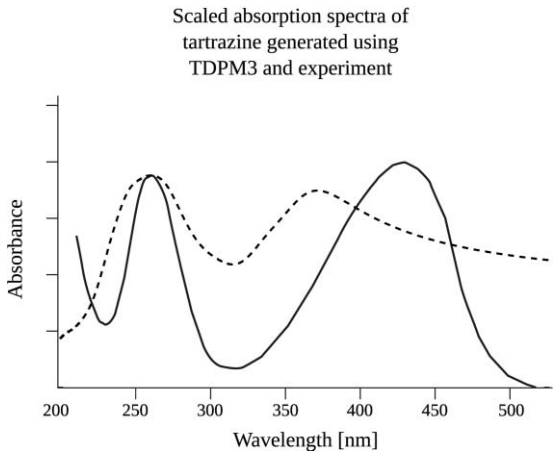

FIG. 10. Overlay of the TDPM3-generated (dashed line) and experimentally generated (solid line) absorbance spectra of tartrazine.

Figure 9 shows the energy transfer between the second and third nanoparticles for system with and without a molecule around the absorption band of tartrazine and silver. The graph indicates the large decrease in energy transfer, about 65%, at and around the silver plasmon resonance in the presence of the molecule.

Comparing to previous work on a two-level molecular system (Ref. 12), we note several differences.

Percentage-wise, tartrazine has a stronger effect on the current on the third nanoparticle than does the two-level molecule, where the overall current changes by as much as 35%. However, the shape of the curve changes less strongly here: tartrazine results in a reduction of current transfer less sharply pronounced around the excitation energy of the molecule. We attribute this difference to several factors. Mainly, tartrazine does not have as sharp an absorbance as the two-level molecule. Also, Fig. 4 shows that tartrazine has several excitation modes at or near silver's plasmon frequency. This leads to differences in absorption and re-emission.

These main differences arise from the fact that the properties of the two-level molecule were tunable, i.e., we were able to set the excitation frequency and more importantly the extinction coefficient. In contrast, the properties of tartrazine are determined by the physics of the molecule itself.

Finally, recall that the absorption of tartrazine in this work is determined by the minimum basis TDPM3 method. While the TDPM3-generated absorption spectrum is qualitatively similar to the experimentally generated absorption spectrum, the differences could change the effects on current transmission between the nanoparticles (see Fig. 10 for an overlay of TDPM3-generated and experimentally generated spectra; experimental spectrum is taken from Ref. 19).

IV. CONCLUSIONS

To conclude, we show the strong effect a single molecule can have on the transmission of current and energy between neighboring nanoparticles.

The presence of tartrazine results in a large decrease in the *x*-polarized current on the third nanoparticle. This current is rotated into the *y*-direction, and we observe *y*-polarized current on the third nanoparticle where none is found without the molecule. This effect can potentially have a multitude of applications in the areas of sensing and molecular switches. The enhancement of *y*-polarized current is sufficient so that devices sensitive enough to detect a single molecule could be conceived.

There are several directions for future research, such as enhancing the effect of a single molecule. This could be achieved with an alternate, more strongly absorbing molecule or by a varied geometry. Another direction could be including more molecules, which could greatly enhance *y*-polarized current on the third nanoparticle or cause a resonant effect between the molecules.

The present work is a multiscale approach to model the interaction between molecules and metal surfaces. The method allows a simultaneous treatment of a quantum mechanical molecule interacting with a classical metal cluster. This combined approach allows for an accurate treatment of the respective components in the system without sacrificing efficiency.

The approach developed here is general. Because the interface between the classical FDTD routine and the TDPM3 routine does not depend on either specifically, other methods could be substituted. For example, the model could easily account for the introduction of TDDFT as an alternative to TDPM3. In addition, the fact that the metals are described by just a few parameters, substitution of any metal for which the necessary experimental data is available is possible.

An extension of the present work will be the modeling of complex molecule–metal surface interactions. A future direction would be a more sophisticated interface between the molecule(s) and metal.

ACKNOWLEDGMENTS

We are grateful for the support from the National Science Foundation. We also thank the referees for suggesting specific applications of this concept.

[1] A. J. Haes, C. L. Haynes, A. D. McFarland, G. C. Schatz, R. P. V. Duyne, and S. Zou, MRS Bull. **30**, 368 (2005).
[2] W. A. Murray and W. L. Barnes, Adv. Mater. **19**, 3771 (2007).
[3] S. Link and M. A. El-Sayed, J. Phys. Chem. B **103**, 4212 (1999).
[4] C. Burda, X. Chen, R. Narayanan, and M. A. El-Sayed, Chem. Rev. **105**, 1025 (2005).
[5] S. A. Maier, P. G. Kik, and H. A. Atwater, Appl. Phys. Lett. **81**, 1714 (2002).
[6] S. A. Maier, P. G. Kik, H. A. Atwater, S. Meltzer, E. Harel, B. E. Koel, and A. A. G. Requicha, Nature Mater. **2**, 229 (2003).
[7] L. Yin, V. K. Vlasko-Vlasov, J. Pearson, J. M. Hiller, J. Hua, U. Welp, D. E. Brown, and C. W. Kimball, Nano Lett. **5**, 1399 (2005).
[8] J. Dintinger, S. Klein, and T. W. Ebbesen, Advanced Mat. **18**, 1267 (2006).
[9] S. Nie and S. R. Emory, Science **275**, 1102 (1997).
[10] S. Mackowski, S. Wormke, A. J. Maier, T. H. P. Brotosudarmo, H. Harutyunyan, A. Hartschuh, A. O. Govorov, H. Scheer, and C. Brauchle, Nano Lett. **8**, 558 (2007).
[11] J. Zhao, L. Jensen, J. Sung, S. Zou, G. C. Schatz, and R. P. Van Duyne, J. Am. Chem. Soc. **129**, 7647 (2007).

[12]K. Lopata and D. Neuhauser, J. Chem. Phys. **130**, 104707 (2009).
[13]D. Neuhauser and K. Lopata, J. Chem. Phys. **127**, 154715 (2007).
[14]A. Taflove and S. C. Hagness, *Computational Electrodynamics: The Finite-Difference Time-Domain Method* (Artech House, Boston, 2005).
[15]S. K. Gray and T. Kupka, Phys. Rev. B **68**, 045415 (2003).
[16]J. J. P. Stewart, J. Comp. Chem. **10**, 209 (1989).
[17]L. A. Bartell, M. R. Wall, and D. Neuhauser, J. Chem. Phys. **132**, 234106 (2010).
[18]A. Vial, A.-S. Grimault, D. Macías, D. Barchiesi, and M. L. de la Chapelle, Phys. Rev. B **71**, 085416 (2005).
[19]V. L. Bagirova and L. I. Mit'kina, Pharm. Chem. J. **37**, 558 (2003).